

CLINICAL AND POPULATION SCIENCES

# Effect of Osteoporotic Condition on Ventriculomegaly and Shunt-Dependent Hydrocephalus After Subarachnoid Hemorrhage

Yu Deok Won, MD; Jae Min Kim, MD, PhD; Jin Hwan Cheong, MD, PhD; Je Il Ryu, MD, PhD; Hyeong-Joong Yi, MD, PhD; Myung-Hoon Han<sup>1</sup>, MD, PhD

**BACKGROUND AND PURPOSE:** Hydrocephalus is a common complication in aneurysmal rupture subarachnoid hemorrhage (SAH). As both the bone and arachnoid trabeculae are composed of type 1 collagen, we identified the possible relationship between bone mineral density and ventriculomegaly and shunt-dependent hydrocephalus (SDHC) development after aneurysmal rupture SAH in younger patients.

**METHODS:** We measured frontal skull Hounsfield unit (HU) values on brain computed tomography upon admission, and mean frontal skull HU values were used instead of T-score value. Hazard ratios were calculated using Cox regression analysis to identify whether osteoporotic condition is an independent predictor for ventriculomegaly and SDHC after surgical clipping for SAH in younger patients.

**RESULTS:** Altogether, 412 patients ( $\leq 65$  years) who underwent surgical clipping for primary spontaneous SAH from a ruptured aneurysm were enrolled in this 11-year analysis in 2 hospitals. We observed that the first tertile group of skull HU was an independent predictor of SDHC after SAH compared with the third tertile of skull HU values (hazard ratio, 2.55 [95% CI, 1.25–5.20];  $P=0.010$ ). There were no significant interactions between age and skull HU with respect to ventriculomegaly and SDHC in younger patients.

**CONCLUSIONS:** Our study suggests a relationship between possible osteoporotic conditions and ventriculomegaly and SDHC development after SAH in younger patients. Our findings may be useful in predicting hydrocephalus in young SAH patients using a convenient method of measuring skull HU value on brain computed tomography upon admission.

**Key Words:** bone density ■ hospitals ■ hydrocephalus ■ skull ■ subarachnoid hemorrhage

Hydrocephalus is a common complication in subarachnoid hemorrhage (SAH) caused by aneurysmal rupture, and the percentage of shunt-dependent hydrocephalus (SDHC) occurrence after SAH is  $\approx 20\%$  to  $30\%$ .<sup>1</sup> Patients with SDHC after SAH experience cognitive and functional impairment, and there is no reliable preventive treatment for SDHC after SAH.<sup>2</sup> Therefore, identifying risk factors for hydrocephalus after SAH is crucial, and tools to predict SDHC development are necessary to minimize chronic hydrocephalus-related complications.<sup>2</sup>

As both the bone and arachnoid trabeculae are composed of the type 1 collagen, we previously hypothesized that low bone mineral density (BMD) would negatively affect the integrity of the arachnoid trabeculae and the bone.<sup>3,4</sup> This mechanism may be related to hydrocephalus development after SAH.

We previously showed a strong correlation between the mean frontal skull Hounsfield unit (HU) value and T score.<sup>4,5</sup> Therefore, to assess this postulation, we measured HU values in the cancellous bone of the frontal

Correspondence to: Myung-Hoon Han, MD, PhD, Department of Neurosurgery, Hanyang University Guri Hospital, 153 Gyeongchun-ro, Guri 471-701, Gyonggi-do, Korea. Email gksmh80@gmail.com

The Data Supplement is available with this article at <https://www.ahajournals.org/doi/suppl/10.1161/STROKEAHA.120.031044>.

For Sources of Funding and Disclosures, see page 1003.

© 2021 American Heart Association, Inc.

Stroke is available at [www.ahajournals.org/journal/str](http://www.ahajournals.org/journal/str)

### Nonstandard Abbreviations and Acronyms

<b>BCI</b>	bicaudate index
<b>BMD</b>	bone mineral density
<b>CSF</b>	cerebrospinal fluid
<b>CT</b>	computed tomography
<b>EI</b>	Evans index
<b>HU</b>	Hounsfield unit
<b>SAH</b>	subarachnoid hemorrhage
<b>SDHC</b>	shunt-dependent hydrocephalus

skull, and mean frontal skull HU values were used here instead of the T-score value.

The overall objective of the study was to identify the possible relationship between BMD and hydrocephalus development after SAH. Therefore, the main analysis was performed in younger patients (additional exploratory analyses were also performed including elderly [ $>65$  years] patients) because old age may also contribute to both hydrocephalus development after SAH and low BMD status. Moreover, for a more detailed analysis of hydrocephalus after SAH, we included both the ventricle size, assessed using the bicaudate index (BCI) and Evans index (EI), and the SDHC as dependent variables for the analysis. Patients aged  $\geq 65$  years are commonly referred to as elderly in previous studies of SAH.<sup>6,7</sup> In addition, according to the several studies, the upper limit of normal (95th percentile) for BCI in SAH patients without concurrent hydrocephalus is changed between  $\leq 65$  years and  $>65$  years.<sup>8,9</sup> Therefore, in the study, we defined the younger patients as those aged  $\leq 65$  years.

## METHODS

The data that support the findings of this study are available from the corresponding author upon reasonable request.

### Study Patients

We retrospectively investigated data of all consecutive primary aneurysmal rupture SAH patients ( $>18$  years old) who underwent surgical clipping from the Registry of Hemorrhagic Stroke Patients of the Department of Neurosurgery of Hanyang University Medical Center (Seoul and Guri) from January 1, 2008, to December 31, 2018. All coiling cases were excluded as clipping was preferred for SAH patients at the Guri Hospital. This may reduce the possible effect of treatment heterogeneity on the hydrocephalus occurrence after SAH.

Altogether, 649 patients were initially identified, and 135 were excluded for the following reasons: (1) absence of follow-up computed tomography (CT) images after aneurysmal clipping (13 patients), (2) early death (within 2 weeks) after clipping for SAH (85 patients), (3) postoperative hemorrhagic complications (15 patients), and (4) no measurable cancellous bone (too narrow intercortical space of the frontal skull;

22 patients). The remaining 514 patients from the 2 hospitals were included. However, as described in the Introduction, the statistical analysis was mainly focused on young patients ( $\leq 65$  years) because BMD strongly correlates with age, and the prevalence of either low BMD or osteoporosis is higher in older patients.<sup>10</sup> Excluding older patients may reduce the possible effect of age on the BMD for predicting hydrocephalus development in SAH patients.

This study was approved by the Institutional Review Boards of the Hanyang University Medical Center in both Seoul and Guri and conformed with the tenets of the Declaration of Helsinki. As this was a retrospective study, the requirement for informed consent was waived. All individual records were anonymized before analysis.

### Surgical Treatment and Management for SAH

Three faculty neurosurgeons (H.-J.Y. in Seoul, and J.M.K. and J.H.C. in Guri) performed all operations, using the same surgical techniques and management because they were all previously trained by the same senior neurosurgeon at the same hospital. All SAH patients were treated with the standard SAH treatment protocol including intracranial pressure control (mannitol or glycerol), triple-H (hypervolemia/hypertension/hemodilution) therapy, and administration of nimodipine and an anticonvulsant agent. Ventriculoperitoneal shunt was performed when the patient showed ventricular enlargement (BCI  $>0.2$  or EI  $>0.3$ ) on brain CT scan with hydrocephalus-related symptoms. Hydrocephalus-related symptoms were defined as neurological deterioration such as aggravated response to painful stimuli, particularly in unconscious patients, and development or aggravation of confusion, gait disturbance, or urinary incontinence, particularly in conscious patients.

### Baseline and Follow-Up Images

We obtained all CT images (4.0–5.0-mm slice thicknesses) with Philips and Siemens CT scanners in both hospitals. A previous study demonstrated that variations in HU values are small (0–20 HU) between Philips and Siemens CT scanners.<sup>11</sup> The baseline CT image was obtained in the emergency room upon SAH diagnosis. We included 1 follow-up CT image per individual. To assess ventricle size change within 1 year from the time of surgical clipping for SAH, we defined the follow-up CT image as the last follow-up CT closest to 1-year postclipping for SAH. When the patients had lumbar or external ventricular cerebrospinal fluid (CSF) drainage or ventriculoperitoneal shunt insertion within 1 year after clipping, we included the follow-up CT images, which were taken immediately before such procedures.

### Measurement of the Skull HU Values and Assessment of Ventricular Enlargement

We previously described detailed methods for measuring HU values on the frontal cancellous bone on brain CT scan at the point where the lateral ventricles disappear (Figure I in the [Data Supplement](#)).<sup>4,5</sup> We measured HU values at each of the four lines on the frontal cancellous bone (right lateral, right medial, left medial, and left lateral) between the right and left coronal sutures. All CT images were also magnified for HU measurement to minimize measurement errors.

To assess ventricle size changes after SAH, we measured the BCI and EI using both baseline and follow-up CT images (Figure II in the [Data Supplement](#)). The BCI was measured by dividing the width of 2 lateral ventricles at the level of the head of the caudate nucleus by the corresponding diameter of the brain along the same line.<sup>9,12</sup> The EI was defined as the maximum width of the frontal horns of the lateral ventricles divided by the maximal transverse inner diameter of the cranium at the same level of axial brain CT.<sup>13</sup> All measurements of the skull HU, BCI, and EI were conducted blindly to the patients' clinical data.

### Clinical and Radiographic Factors

All enrolled patients' clinical information such as sex, age, performance of external CSF drainage and ventriculoperitoneal shunt, Hunt and Hess grade, operation type, hypertension, and diabetes was investigated from medical and operative records. Radiographic factors associated with SAH were also evaluated including Fisher grade, aneurysm location, intracerebral hemorrhage, and intraventricular hemorrhage. Vasospasm was defined as angiographic spasms confirmed by follow-up digital subtraction angiography, CT angiography, or perfusion CT with neurological symptoms.

### Statistical Methods

The  $\chi^2$  and Student *t* test were conducted to evaluate differences between both age groups. Statistical analysis was conducted in younger patients ( $\leq 65$  years). The mean skull HU value (sum of the mean right lateral, right medial, left medial, and left lateral HU values divided by 4) was used in all analyses. The skull HU values in younger patients were classified into tertile groups and were analyzed, namely, first (HU,  $\leq 724.5$ ;  $n=137$ ), second (HU, 724.6–963.3;  $n=137$ ), and third (HU,  $>963.3$ ;  $n=138$ ) tertiles. Statistical comparison between skull HU tertile groups was performed using 1-way ANOVA test.

A scatterplot with a linear regression line or a line determined by a locally weighted scatterplot smoothing was used to graphically represent the association between several variables. The rationale and detailed methods underlying the use of locally weighted scatter plot smoothing were described previously.<sup>14</sup> Box plots with dot plots were used to visualize BCI and EI differences between the skull HU tertile groups based on the tertile groups of days from surgical clipping for SAH.

The cumulative hazards for ventricular enlargement and SDHC were examined using the Kaplan-Meier analysis classified by tertile groups of skull HU values. Hazard ratios with 95% CIs were then estimated with uni- and multivariate Cox regression analyses to evaluate independent predictive factors for ventriculomegaly and SDHC after surgical clipping for SAH. We also performed interaction analysis between age and skull HU regarding ventriculomegaly and SDHC.

$P < 0.05$  was considered statistically significant. All statistical analyses were performed using R software, version 3.6.3, and SPSS for Windows, version 24.0, software (IBM, Chicago, IL).

## RESULTS

### Patient Characteristics and Selection

Altogether, 514 consecutive patients ( $>18$  years old) alive  $\geq 2$  weeks who underwent surgical clipping for primary

spontaneous SAH due to a ruptured aneurysm were enrolled in this 11-year study in 2 hospitals. The mean patient age was 55.1 years, and 412 (80.2%) patients belonged to the younger age group ( $\leq 65$  years). There were significant differences in baseline and follow-up ventricle size and SDHC occurrence between both groups. Detailed information of the study patients is shown in Table 1. We observed a stronger negative correlation between age and skull HU values in overall patients than in younger patients (Figure III in the [Data Supplement](#)). Additionally, there were significant differences in skull HU values according to ventriculomegaly and SDHC in all patients and those in the younger age group (Figure IV in the [Data Supplement](#)). As described above, the main analysis was performed in younger patients to reduce the interaction between age and possible BMD with respect to ventriculomegaly or SDHC.

### Skull HU Values According to Ventriculomegaly and SDHC in Younger Patients

Table 2 shows descriptive statistics of detailed frontal skull HU values according to ventriculomegaly and SDHC after surgical clipping for SAH. The overall average mean frontal skull HU value was 835.9, and there were significant differences in mean frontal skull HU values and distribution of skull HU tertile groups according to ventriculomegaly and SDHC.

### Trend in Ventricle Size Change After SAH According to Skull HU Tertile Groups in Younger Patients

As this was a retrospective study, it was unfeasible to represent the precise natural course of ventricle size changes after SAH. However, after the BCI and EI values were randomly evaluated within 1 year after SAH, we observed different trends in ventricle size change from SAH according to skull HU tertile groups in younger patients. The highest tertile group of skull HU showed the lowest increase in ventricle size during the rapid ventricular growing period  $\approx 2$  to 3 months after SAH (Figure 1A and 1B). When we divided days from clipping for SAH into tertile groups, there were significant differences in ventricle size after SAH between skull HU tertile groups in the second tertile of days from clipping for SAH (Figure 1C and 1D).

### Cumulative Hazard of Ventriculomegaly and SDHC After SAH According to Skull HU Tertile Groups in Younger Patients

Patients in the first tertile skull HU value group showed significantly greater ventriculomegaly development within 1 year after SAH than those in the second and third tertile groups in younger patients (Figure 2A through 2C). Similarly, patients with lower skull HU values showed a

**Table 1. Characteristics of Patients With Primary Spontaneous Subarachnoid Hemorrhage Who Underwent Surgical Clipping Classified According to Age Group**

Characteristics	Age ≤65 y	Age >65 y	Total	P value
n	412 (80.2%)	102 (19.8%)	514	
Sex: female, n (%)	203 (49.3)	55 (53.9)	258 (50.2)	0.439
Age, y; mean±SD	50.7±8.1	73.2±5.2	55.1±11.8	<0.001
Time interval between clipping and shunting, d; median (IQR)	52.5 (34.0–85.3)	53.0 (35.0–73.0)	53.0 (34.0–76.0)	0.336
Ventriculoperitoneal shunt, n (%)	62 (15.0)	29 (28.4)	91 (17.7)	0.002
Time interval between clipping and follow-up image, d; median (IQR)	91.0 (30.3–177.8)	49.5 (18.0–99.8)	88.0 (24.0–168.3)	0.008
Baseline BCI, mean±SD	0.145±0.04	0.178±0.04	0.151±0.04	<0.001
Baseline EI, mean±SD	0.253±0.04	0.274±0.03	0.257±0.04	<0.001
Baseline ventricular enlargement, n (%)				
BCI >0.2	37 (9.0)	28 (27.5)	65 (12.6)	<0.001
EI >0.3	39 (9.5)	18 (17.6)	57 (11.1)	0.023
BCI >0.2 and EI >0.3	20 (4.9)	12 (11.8)	32 (6.2)	0.019
Follow-up BCI, mean±SD	0.167±0.06	0.190±0.06	0.172±0.06	<0.001
Follow-up EI, mean±SD	0.283±0.05	0.294±0.05	0.286±0.05	0.065
Follow-up ventricular enlargement, n (%)				
BCI >0.2	101 (24.5)	47 (46.1)	148 (28.8)	<0.001
EI >0.3	133 (32.3)	48 (47.1)	181 (35.2)	0.008
BCI >0.2 and EI >0.3	92 (22.3)	39 (38.2)	131 (25.5)	0.001
Mean frontal skull HU, mean±SD	875.0±274.3	652.2±265.0	830.8±286.4	<0.001
Classification of the skull HU based on tertile groups, HU				
Tertile 1	≤724.5	≤534.5	≤685.8	
Tertile 2	724.6–963.3	534.6–685.8	685.9–927.3	
Tertile 3	>963.3	>685.8	>927.3	
Hunt-Hess grade, n (%)				0.112
Grade 1	23 (5.6)	6 (5.9)	29 (5.6)	
Grade 2	214 (51.9)	38 (37.3)	252 (49.0)	
Grade 3	105 (25.5)	36 (35.3)	141 (27.4)	
Grade 4	66 (16.0)	21 (20.6)	87 (16.9)	
Grade 5	4 (1.0)	1 (1.0)	5 (1.0)	
Modified Fisher grade, n (%)				0.023
1	80 (19.4)	14 (13.7)	94 (18.3)	
2	35 (8.5)	8 (7.8)	43 (8.4)	
3	127 (30.8)	21 (20.6)	148 (28.8)	
4	170 (41.3)	59 (57.8)	229 (44.6)	
Location, n (%)				0.014
ACA	150 (36.4)	27 (26.5)	177 (34.4)	
MCA	134 (32.5)	32 (31.4)	166 (32.3)	
ICA	26 (6.3)	2 (2.0)	28 (5.4)	
PCOM	95 (23.1)	39 (38.2)	134 (26.1)	
VBA	7 (1.7)	2 (2.0)	9 (1.8)	
IVH, n (%)	135 (32.8)	45 (44.1)	180 (35.0)	0.037
ICH, n (%)	112 (27.2)	32 (31.4)	144 (28.0)	0.392
Craniectomy, n (%)	58 (14.1)	10 (9.8)	68 (13.2)	0.327
Vasospasm, n (%)	128 (31.1)	24 (23.5)	152 (29.6)	0.147
Hypertension, n (%)	145 (35.2)	50 (49.0)	195 (37.9)	0.012
Diabetes, n (%)	27 (6.6)	16 (15.7)	43 (8.4)	0.005

ACA indicates anterior cerebral artery; BCI, bicaudate index; EI, Evans index; HU, Hounsfield unit; ICA, internal carotid artery; ICH, intracerebral hemorrhage; IQR, interquartile range; IVH, intraventricular hemorrhage; MCA, middle cerebral artery; PCOM, posterior communicating artery; and VBA, vertebrobasilar artery.

Downloaded from <http://ahajournals.org> by on March 19, 2023

**Table 2. Descriptive Statistics of Frontal Skull HU Values in Younger Patients (≤65 Years) Classified According to Ventricular Enlargement (Simultaneous Bicaudate Index >0.2 and Evans Index >0.3) and SDHC After Aneurysmal Clipping for Subarachnoid Hemorrhage**

Characteristics	Overall	Ventricular enlargement– (n=320)	Ventricular enlargement+ (n=92)	P value	SDHC– (n=350)	SDHC+ (n=62)	P value
Overall mean frontal skull HU value, median (IQR)	835.9 (684.3–1038.5)	855.8 (691.8–1062.2)	771.6 (662.3–943.3)	0.045	849.4 (695.8–1050.5)	749.4 (635.9–931.4)	0.018
Overall mean frontal skull HU value, mean±SD	875.0±274.3	889.5±274.7	824.4±268.2	0.045	888.4±276.9	799.1±247.1	0.018
Mean HU value at each of the 4 sites in the frontal skull, mean±SD							
Right lateral	795.0±266.2	807.6±262.2	751.1±276.8	0.073	807.7±269.5	723.0±236.6	0.021
Right medial	954.6±308.0	965.5±309.8	916.8±300.1	0.181	964.7±310.7	897.4±288.0	0.113
Left medial	944.9±314.8	959.9±315.2	892.4±309.4	0.070	959.8±318.3	860.4±282.1	0.022
Left lateral	805.6±266.4	825.2±267.7	737.3±251.2	0.005	821.5±268.3	715.6±237.8	0.004
Average, medial	949.7±305.5	962.7±306.5	904.6±299.4	0.108	962.3±308.4	878.9±280.6	0.048
Average, lateral	800.3±259.9	816.4±258.9	744.2±256.9	0.019	814.6±262.2	719.3±232.2	0.008
Classification of the skull HU based on tertile groups, n (%)				0.017			0.023
Tertile 1 (HU, ≤724.5)	137 (33.3)	98 (30.6)	39 (42.4)		109 (31.1)	28 (45.2)	
Tertile 2 (HU, 724.6–963.3)	137 (33.3)	104 (32.5)	33 (35.9)		115 (32.9)	22 (35.5)	
Tertile 3 (HU, >963.3)	138 (33.5)	118 (36.9)	20 (21.7)		126 (36.0)	12 (19.4)	

HU indicates Hounsfield unit; IQR, interquartile range; and SDHC, shunt-dependent hydrocephalus.

higher rate of SDHC development in the clinical course of SAH (Figure 2D;  $P=0.016$ ).

### Independent Predictive Factors for Ventriculomegaly and SDHC Development After SAH in Younger Patients

Multivariate Cox regression analysis showed the first and second tertile groups of the skull HU as independent predictors of ventriculomegaly (simultaneous BCI >0.2 and EI >0.3) after SAH compared with those in the highest tertile group in younger patients (hazard ratio, 2.92 [95% CI, 1.62–5.30];  $P<0.001$ ; hazard ratio, 2.30 [95% CI, 1.26–4.22];  $P=0.007$ , respectively; Table 3). Moreover, the first tertile group of skull HU was also an independent predictive factor of SDHC after surgical clipping for SAH compared with the third tertile of skull HU values (hazard ratio, 2.55 [95% CI, 1.25–5.20];  $P=0.010$ ). Other independent predictors of both ventriculomegaly and SDHC were higher Hunt-Hess grade, ventriculomegaly on admission, and accompanying intraventricular hemorrhage. Decompressive craniectomy was an independent predictor only in the ventriculomegaly after SAH. We also present the univariate Cox regression analysis result in Table I in the [Data Supplement](#).

### Interaction Analysis Between Age and Skull HU Values With Respect to Ventriculomegaly and SDHC in Younger Patients

Because age is correlated with BMD, we initially excluded older patients (>65 years) from the analysis and adjusted

age with continuous variables in the multivariate analysis. However, we further performed interaction analysis between age and skull HU with respect to ventriculomegaly and SDHC after SAH in younger patients. However, there were no significant interactions between age and skull HU values with respect to ventriculomegaly and SDHC in younger patients (Figure 3).

### Additional Analysis to Assess the Effect of Age on the Results

We performed additional analysis including elderly (>65 years) patients to evaluate the effect of old age on the association between possible osteoporotic conditions and ventriculomegaly and SDHC after SAH. We observed similar and more significant differences in ventriculomegaly and SDHC after SAH among the skull HU tertile groups (Figures V and VI in the [Data Supplement](#)). Expectedly, when we performed uni- and multivariate regression analysis, we observed stronger influence of age on possible osteoporotic conditions and hydrocephalus after SAH than that in the results of studies including only younger patients (Tables II and III in the [Data Supplement](#)). However, although the association between the first tertile group of skull HU and SDHC was slightly short of significance ( $P=0.056$ ), the effect of possible osteoporotic conditions on ventriculomegaly and SDHC after SAH was maintained after adjusting for all variables, including age in all (included >65 years) patients (Table III in the [Data Supplement](#)). There were no significant interactions between age and skull HU

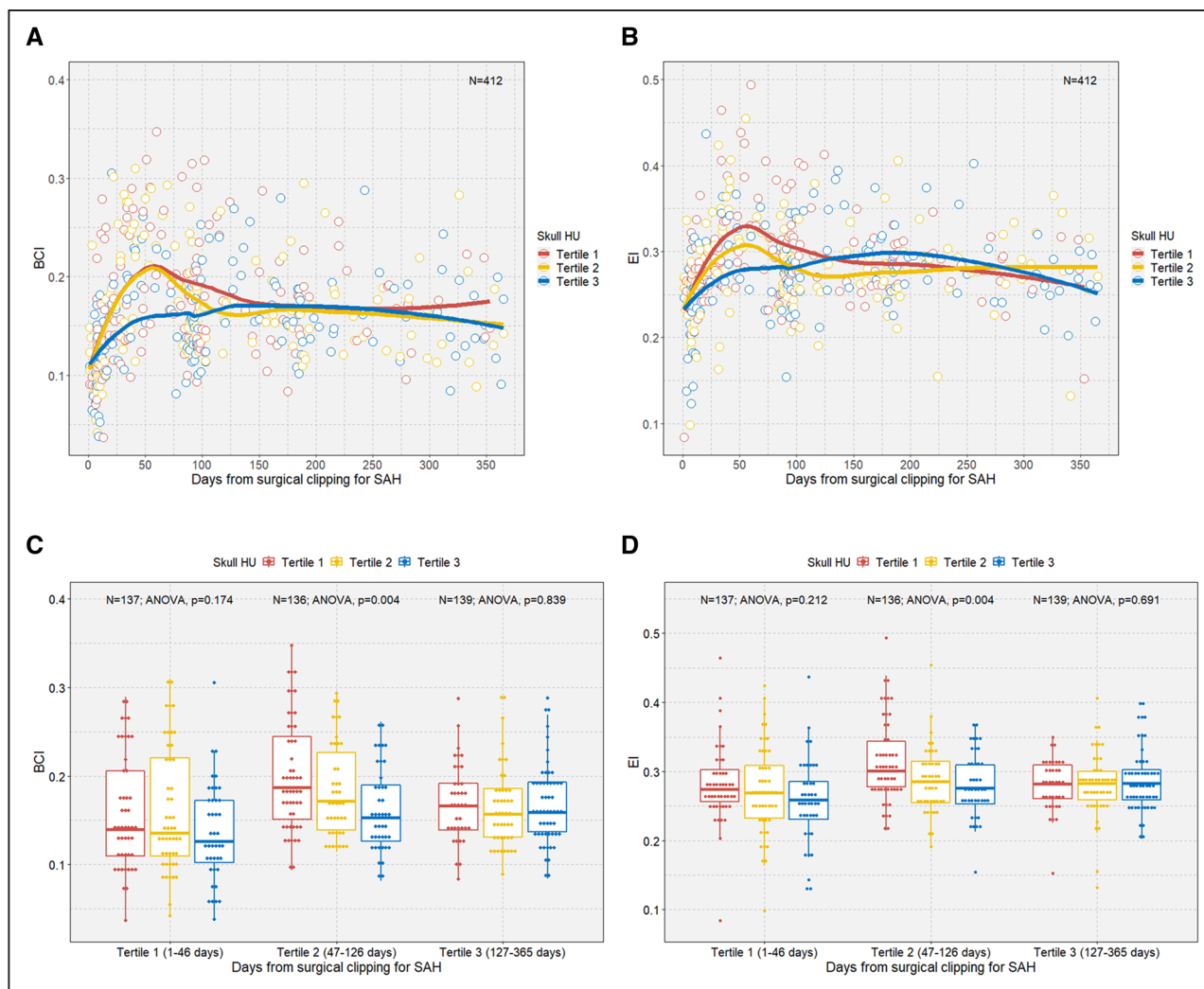


**Figure 1. Trend in ventricle size change after subarachnoid hemorrhage (SAH) according to tertile groups of skull Hounsfield unit (HU) in younger patients.**

**A**, Scatterplot with locally weighted scatter plot smoothing (LOWESS) curve showing the trend between days after surgical clipping for SAH and the bicaudate index (BCI) according to tertile groups of mean frontal skull HU values. **B**, Scatterplot with LOWESS curve showing the trend between days after surgical clipping for SAH and the Evans index (EI) according to tertile groups of mean frontal skull HU values. **C**, Box plots with dot plots showing the trend between tertile groups of days after surgical clipping for SAH and the BCI according to tertile groups of mean frontal skull HU values. **D**, Box plots with dot plots showing the trend between tertile groups of days after surgical clipping for SAH and the EI according to tertile groups of mean frontal skull HU values.

with respect to ventriculomegaly and SDHC among all patients (Figure VII in the [Data Supplement](#)).

## DISCUSSION

Our study showed that possible low BMD is associated with a more increased risk of ventricular enlargement and SDHC development after surgical clipping for SAH compared with the possible higher BMD group after adjusting for other risk factors, including age in younger patients ( $\leq 65$  years). Therefore, we suggest that low BMD state or osteoporotic condition is independently more associated with hydrocephalus development in the clinical course of SAH among younger patients.

An HU is an accurate and absolute value on any anatomic region on a CT image, and the HU value of bone reportedly ranges from 300 to 3000.<sup>15</sup> Previous studies demonstrated that cancellous bone HU values on specific regions from CT scans are strongly associated with T score, and HU values of cancellous bone may be useful for predicting osteoporotic conditions.<sup>15-17</sup> We also previously reported a strong correlation between skull HU values and T score, and the HU value of the frontal skull cancellous bone may be predictive of osteoporotic conditions.<sup>4,5</sup> Although in a previous study, we showed a considerable scattering plot between the T score and skull HU value, the receiver operating characteristic curve analysis with a large sample size showed >70% specificity and sensitivity of the mean skull HU for prediction of

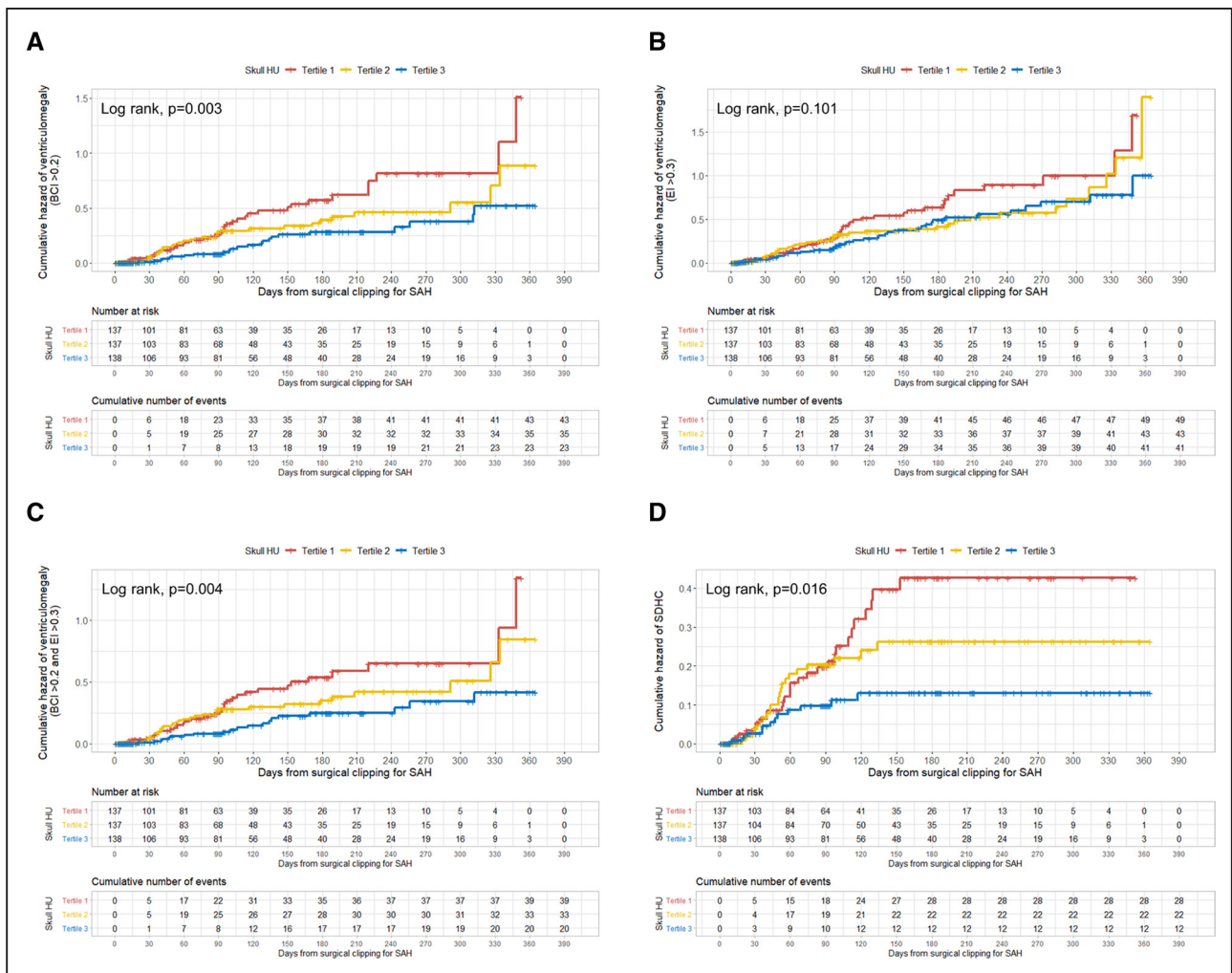


**Figure 2. Kaplan-Meier curves showing the cumulative hazard for ventriculomegaly and shunt-dependent hydrocephalus (SDHC) after subarachnoid hemorrhage (SAH) in younger patients.**

**A**, Cumulative hazard of ventriculomegaly (bicaudate index [BCI], >0.2) according to tertile groups of skull Hounsfield unit (HU) values. **B**, Cumulative hazard of ventriculomegaly (Evans index [EI], >0.3) according to tertile groups of skull HU values. **C**, Cumulative hazard of ventriculomegaly (simultaneous BCI >0.2 and EI >0.3) according to tertile groups of skull HU values. **D**, Cumulative hazard of SDHC according to tertile groups of skull HU values.

osteopenia and osteoporosis.<sup>4</sup> Because osteoporosis is a systemic disease that is strongly associated with genetic components of type 1 collagen such as *COL1A1* and *COL1A2*, cancellous bone structures in the skull may be also affected by osteoporotic conditions.

Type 1 collagen is a major component of the bone, and its gene mutation leads to low BMD and osteoporosis.<sup>18,19</sup> Therefore, it may be strongly associated with osteoporotic conditions. Interestingly, both the arachnoid trabeculae and granulations are also composed of type 1 collagen.<sup>3</sup> The arachnoid trabeculae composed of abundant strands of collagen tissue are important as mechanical pillars between the pia and arachnoid membranes to support the stability of the subarachnoid space and CSF flow.<sup>20</sup> The curtain-like structure of the subarachnoid trabeculae has holes through which CSF flows, and structural changes due to hemorrhage could contribute to posthemorrhagic hydrocephalus.<sup>20</sup> Therefore, as we

reported previously, systemic osteoporosis may negatively influence the structural integrity of arachnoid trabeculae because both the bone and arachnoid trabeculae are composed of the type 1 collagen.<sup>4</sup> Supporting our hypothesis, osteogenesis imperfecta caused by mutations in type 1 collagen genes (*COL1A1*/*COL1A2*) is associated with communicating hydrocephalus.<sup>21</sup> Therefore, our results may be explained by the following hypothetical mechanism: when SAH occurred, the weaker subarachnoid trabeculae due to osteoporotic conditions may be more damaged from hemorrhage, which may lead to an increased risk of hydrocephalus development after SAH. Further, our study, which focused on younger patients, may be valuable to identify the association between BMD and hydrocephalus development after SAH because possible effect of old age on both hydrocephalus development and BMD status may be reduced. Additionally, we included both ventricle size and SDHC

**Table 3. Multivariate Cox Regression Analyses of Ventriculomegaly (Simultaneous BCI >0.2 and EI >0.3) and SDHC After Aneurysmal Clipping for Subarachnoid Hemorrhage Based on Predictive Factors in Younger Patients (≤65 Years)**

Variable	Ventriculomegaly		SDHC	
	HR (95% CI)	P value	HR (95% CI)	P value
Sex				
Male	Reference		Reference	
Female	1.09 (0.70–1.70)	0.710	1.33 (0.78–2.28)	0.297
Age, y (per 1-y increase)	1.03 (1.00–1.05)	0.089	1.03 (1.00–1.07)	0.060
Tertile groups of mean frontal skull HU				
Tertile 1	2.92 (1.62–5.30)	<0.001	2.55 (1.25–5.20)	0.010
Tertile 2	2.30 (1.26–4.22)	0.007	1.80 (0.84–3.87)	0.133
Tertile 3	Reference		Reference	
Hunt-Hess grade				
1–3	Reference		Reference	
4 and 5	2.32 (1.25–4.29)	0.007	3.61 (1.76–7.42)	<0.001
Modified Fisher grade (per 1-point increment)	1.01 (0.77–1.32)	0.969	0.79 (0.57–1.09)	0.149
Ventriculomegaly (BCI >0.2 and EI >0.3) on admission				
No	Reference		Reference	
Yes	4.30 (2.08–8.89)	<0.001	2.65 (1.05–6.70)	0.040
Aneurysm location				
Anterior circulation	Reference		Reference	
Posterior circulation	0.89 (0.51–1.54)	0.667	1.45 (0.80–2.62)	0.224
IVH				
No	Reference		Reference	
Yes	1.75 (1.00–3.07)	0.049	2.28 (1.15–4.50)	0.018
ICH				
No	Reference		Reference	
Yes	0.88 (0.53–1.46)	0.612	0.65 (0.34–1.22)	0.179
Operation type				
Craniotomy	Reference		Reference	
Craniectomy	1.89 (1.01–3.53)	0.045	1.53 (0.74–3.13)	0.251
Vasospasm				
No	Reference		Reference	
Yes	0.96 (0.58–1.60)	0.885	0.93 (0.51–1.70)	0.803
Hypertension				
No	Reference		Reference	
Yes	0.89 (0.54–1.45)	0.629	0.88 (0.48–1.61)	0.676
Diabetes				
No	Reference		Reference	
Yes	0.84 (0.37–1.92)	0.683	1.36 (0.57–3.26)	0.495

BCI indicates bicaudate index; EI, Evans index; HR, hazard ratio; HU, Hounsfield unit; ICH, intracerebral hemorrhage; IVH, intraventricular hemorrhage; and SDHC, shunt-dependent hydrocephalus.

after SAH as dependent variables for the analysis. This may be valuable because not all hydrocephalus patients underwent ventriculoperitoneal shunt due to various reasons including medical problems, financial hardship, or patient's or guardian's decision. Conversely, SDHC patients do not always meet simultaneous BCI >0.2 and EI >0.3 on follow-up brain CT imaging immediately before ventriculoperitoneal shunt insertion.

According to our findings, other possible predictive factors for ventriculomegaly and SDHC after SAH were a higher Hunt-Hess grade, ventriculomegaly upon admission, intraventricular hemorrhage, and decompressive craniectomy. Those variables are reportedly predictive factors for hydrocephalus after SAH.<sup>22,23</sup>

Our study has some limitations. First, due to the study's retrospective nature, time duration between

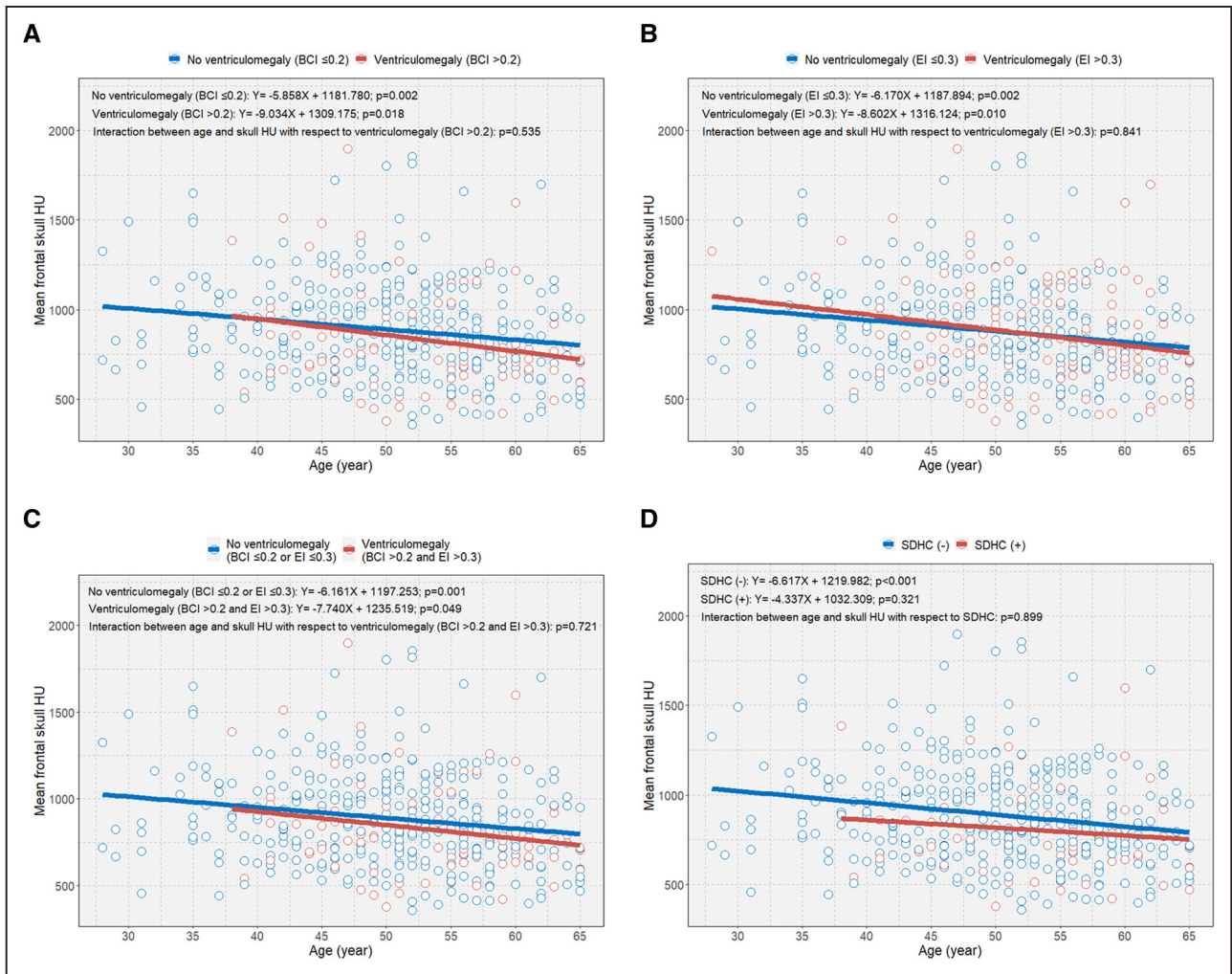


**Figure 3. Interaction plots between age and skull Hounsfield unit (HU) with respect to ventriculomegaly and shunt-dependent hydrocephalus (SDHC) after subarachnoid hemorrhage (SAH).**

**A**, Interaction between age and skull HU with respect to ventriculomegaly (bicaudate index [BCI],  $> 0.2$ ). **B**, Interaction between age and skull HU with respect to ventriculomegaly (Evans index [EI],  $> 0.3$ ). **C**, Interaction between age and skull HU with respect to ventriculomegaly (simultaneous BCI  $> 0.2$  and EI  $> 0.3$ ). **D**, Interaction between age and skull HU with respect to SDHC.

surgical clipping for SAH and follow-up CT image was irregular. However, even in a prospective study, it would be impossible to strictly maintain a regular time interval because of various possible unexpected emergency situations during the early follow-up period of SAH such as sudden neurological deterioration, vasospasm, or emergency external CSF drainage due to hydrocephalus. Second, the actual T score was unavailable for the study patients because evaluating the BMD status is not generally necessary in SAH patients. Although cancellous bone HU values of the frontal skull are strongly correlated with the real BMD, those may not directly reflect the exact T score. Third, measurement errors may have occurred. However, we magnified all brain CT images for HU measurement to exclude cortical bone, and patients with no measurable cancellous bone of the frontal skull were initially excluded for the study. Moreover,

BCI and EI measurements are frequently used, making it familiar to neurosurgeons. Lastly, we included only Korean patients, which may limit the generalizability of results because regional and interracial genetic differences may affect BMD. Therefore, further studies are required to confirm these results.

## CONCLUSIONS

In conclusion, we tried to identify the possible effect of BMD on hydrocephalus occurrence after surgical clipping for SAH. Our study suggests a relationship between possible osteoporotic conditions and ventriculomegaly and SDHC development after SAH in younger patients. Our findings may be useful in predicting hydrocephalus in young SAH patients using a convenient method of measuring cancellous bone HU value of the frontal skull by brain CT imaging upon admission.

## ARTICLE INFORMATION

Received May 26, 2020; final revision received October 4, 2020; accepted November 18, 2020.

## Affiliations

Department of Neurosurgery, Hanyang University Guri Hospital, Gyonggi-do, Korea (Y.D.W., J.M.K., J.H.C., J.I.R., M.-H.H.). Department of Neurosurgery, Hanyang University Medical Center, Seoul, Korea (H.-J.Y.).

## Acknowledgments

Dr Han contributed to the conception and design of the study; Dr Won contributed to the acquisition of data; Dr Han contributed to the analysis, visualization, and interpretation of data; Drs Han and Won contributed to the writing of the paper; Drs Kim, Cheong, Ryu, and Yi contributed to the supervision and critical review of the manuscript.

## Sources of Funding

This work was supported by the research fund of Hanyang University (HY-201900000003370).

## Disclosures

None.

## Supplemental Materials

Tables I–III  
Figures I–VII

## REFERENCES

- Chen S, Luo J, Reis C, Manaenko A, Zhang J. Hydrocephalus after subarachnoid hemorrhage: pathophysiology, diagnosis, and treatment. *Biomed Res Int*. 2017;2017:8584753. doi: 10.1155/2017/8584753
- García S, Torné R, Hoyos JA, Rodríguez-Hernández A, Amaro S, Llull L, López-Rueda A, Enseñat J. Quantitative versus qualitative blood amount assessment as a predictor for shunt-dependent hydrocephalus following aneurysmal subarachnoid hemorrhage. *J Neurosurg*. 2018;131:1743–1750. doi: 10.3171/2018.7.JNS18816
- Saboori P, Sadegh A. Histology and morphology of the brain subarachnoid trabeculae. *Anat Res Int*. 2015;2015:279814. doi: 10.1155/2015/279814
- Han MH, Won YD, Na MK, Kim CH, Kim JM, Ryu JI, Yi HJ, Cheong JH. Association between possible osteoporosis and shunt-dependent hydrocephalus after subarachnoid hemorrhage. *Stroke*. 2018;49:1850–1858. doi: 10.1161/STROKEAHA.118.021063
- Na MK, Won YD, Kim CH, Kim JM, Cheong JH, Ryu JI, Han MH. Opportunistic osteoporosis screening via the measurement of frontal skull Hounsfield units derived from brain computed tomography images. *PLoS One*. 2018;13:e0197336. doi: 10.1371/journal.pone.0197336
- Johansson M, Cesarini KG, Contant CF, Persson L, Enblad P. Changes in intervention and outcome in elderly patients with subarachnoid hemorrhage. *Stroke*. 2001;32:2845–2949.
- Hammer A, Ranaie G, Yakubov E, Erbguth F, Holtmannspoeetter M, Steiner HH, Janssen H. Dynamics of outcome after aneurysmal subarachnoid hemorrhage. *Aging (Albany NY)*. 2020;12:7207–7217. doi: 10.18632/aging.103069
- Hasan D, Lindsay KW, Vermeulen M. Treatment of acute hydrocephalus after subarachnoid hemorrhage with serial lumbar puncture. *Stroke*. 1991;22:190–194. doi: 10.1161/01.str.22.2.190
- Dupont S, Rabinstein AA. CT evaluation of lateral ventricular dilatation after subarachnoid hemorrhage: baseline bicaudate index values [correction of values]. *Neurol Res*. 2013;35:103–106. doi: 10.1179/1743132812Y.0000000121
- Compston JE, McClung MR, Leslie WD. Osteoporosis. *Lancet*. 2019;393:364–376. doi: 10.1016/S0140-6736(18)32112-3
- Birnbaum BA, Hindman N, Lee J, Babb JS. Multi-detector row CT attenuation measurements: assessment of intra- and interscanner variability with an anthropomorphic body CT phantom. *Radiology*. 2007;242:109–119. doi: 10.1148/radiol.2421052066
- Bermel RA, Bakshi R, Tjoa C, Puli SR, Jacobs L. Bicaudate ratio as a magnetic resonance imaging marker of brain atrophy in multiple sclerosis. *Arch Neurol*. 2002;59:275–280. doi: 10.1001/archneur.59.2.275
- Ambarki K, Israelsson H, Wählin A, Birgander R, Eklund A, Malm J. Brain ventricular size in healthy elderly: comparison between Evans index and volume measurement. *Neurosurgery*. 2010;67:94–99; discussion 99.
- Cleveland WS, Devlin SJ. Locally weighted regression: an approach to regression analysis by local fitting. *J Am Stat Assoc*. 1988;83:596–610.
- Schreiber JJ, Anderson PA, Rosas HG, Buchholz AL, Au AG. Hounsfield units for assessing bone mineral density and strength: a tool for osteoporosis management. *J Bone Joint Surg Am*. 2011;93:1057–1063. doi: 10.2106/JBJS.J.00160
- Choi MK, Kim SM, Lim JK. Diagnostic efficacy of Hounsfield units in spine CT for the assessment of real bone mineral density of degenerative spine: correlation study between T-scores determined by DEXA scan and Hounsfield units from CT. *Acta Neurochir (Wien)*. 2016;158:1421–1427. doi: 10.1007/s00701-016-2821-5
- Pickhardt PJ, Pooler BD, Lauder T, del Rio AM, Bruce RJ, Binkley N. Opportunistic screening for osteoporosis using abdominal computed tomography scans obtained for other indications. *Ann Intern Med*. 2013;158:588–595. doi: 10.7326/0003-4819-158-8-201304160-00003
- Gajko-Galicka A. Mutations in type I collagen genes resulting in osteogenesis imperfecta in humans. *Acta Biochim Pol*. 2002;49:433–441.
- Grant SFA, Reid DM, Blake G, Herd R, Fogelman I, Ralston SH. Reduced bone density and osteoporosis associated with a polymorphic Sp1 binding site in the collagen type I  $\alpha 1$  gene. *Nat Genet*. 1996;14:203–205.
- Mortazavi MM, Quadri SA, Khan MA, Gustin A, Suriya SS, Hassanzadeh T, Fahimdanesh KM, Adl FH, Fard SA, Taqi MA, et al. Subarachnoid trabeculae: a comprehensive review of their embryology, histology, morphology, and surgical significance. *World Neurosurg*. 2018;111:279–290. doi: 10.1016/j.wneu.2017.12.041
- Charnas LR, Marini JC. Communicating hydrocephalus, basilar invagination, and other neurologic features in osteogenesis imperfecta. *Neurology*. 1993;43:2603–2608. doi: 10.1212/wnl.43.12.2603
- Hao X, Wei D. The risk factors of shunt-dependent hydrocephalus after subarachnoid space hemorrhage of intracranial aneurysms. *Medicine (Baltimore)*. 2019;98:e15970.
- Sheehan JP, Polin RS, Sheehan JM, Baskaya MK, Kassell NF. Factors associated with hydrocephalus after aneurysmal subarachnoid hemorrhage. *Neurosurgery*. 1999;45:1120–1127; discussion 1127. doi: 10.1097/00006123-199911000-00021